Supplementary Information

Oxidation of methane by a biological dicopper center

Ramakrishnan Balasubramanian[1,*], Stephen M. Smith[1,*], Swati Rawat[2], Liliya A. Yatsunyk[1], Timothy L. Stemmler[2], and Amy C. Rosenzweig[1]

[1]Departments of Biochemistry, Molecular Biology and Cell Biology and of Chemistry, Northwestern University, Evanston, IL 60208.

[2]Department of Biochemistry and Molecular Biology, Wayne State University, School of Medicine, Detroit, Michigan 48201.

*These authors contributed equally to this work.

Table S1. Specific activity values for crude membranes isolated from *M. capsulatus* (Bath) using duroquinol as a reductant.

Research group	Specific activity of as-isolated pMMO membranes (nmol propylene oxide min^{-1} mg^{-1})
Our laboratory	50-200
Dalton and coworkers[1, 2]	19-114
DiSpirito and coworkers[3, 4]	40-86
Chan and coworkers[5]	25-30

1. Basu, P., Katterle, B., Andersson, K. K. & Dalton, H. The membrane-associated form of methane monooxygenase from *Methylococcus capsulatus* (Bath) is a copper/iron protein. *Biochem. J.* **369**, 417-427 (2003).
2. Kitmitto, A., Myronova, N., Basu, P. & Dalton, H. Characterization and structural analysis of an active particulate methane monooxygenase trimer from *Methylococcus capsulatus* (Bath). *Biochemistry* **44**, 10954-10965 (2005).
3. Choi, D. W. *et al*. The membrane-associated methane monooxygenase pMMO and pMMO-NADH:quinone oxidoreductase complex from *Methylococcus capsulatus* Bath. *J. Bacteriol.* **185**, 5755-5764 (2003).
4. Choi, D. W. *et al*. Oxidase, superoxide dismutase, and hydrogen peroxide reductase activities of methanobactin from types I and II methanotrophs. *J. Inorg. Biochem.* **102**, 1571-1580 (2008).
5. Yu, S. S.-F. *et al*. Production of high-quality particulate methane monooxygenase in high yields from *Methylococcus capsulatus* (Bath) with a hollow-fiber membrane bioreactor. *J. Bacteriol.* **185**, 5915-5924 (2003).

Table S2. Summary of Cu EXAFS fitting analysis[a]: sample 1, as-isolated pMMO; sample 2, reconstituted pMMO; sample 3, spmoB; sample 4, spmoB_H48N; sample 5, spmoB_H137,139A.

		Nearest Neighbor Ligand Environments[b]								**Long-Range Ligand Environments**[b]				
Sample	**Fit**	**Atom**[c]	**R(Å)**[d]	**C.N.**[e]	**σ^2**[f]	**Atom**[c]	**R(Å)**[d]	**C.N.**[e]	**σ^2**[f]	**Atom**[c]	**R(Å)**[d]	**C.N.**[e]	**σ^2**[f]	***F'***[g]
1	**1.1**	**O/N**	**1.92**	**1.0**	**1.98**	**Cu**	**2.66**	**0.25**	**6.09**	**C**	**3.93**	**0.60**	**3.82**	**0.21**
		O/N	**2.09**	**2.5**	**4.29**									
	1.2	O/N	1.91	1.0	2.24	C	2.71	1.0	1.27	C	3.92	0.75	4.72	0.30
		O/N	2.09	2.5	4.50									
	1.3[h]	*N_{Im}*	*2.13*	*2*	*4.41*	*Cu*	*2.67*	*0.3*	*5.09*					*0.56*
2	**2.1**	**O/N**	**1.95**	**2.0**	**5.44**	**Cu**	**2.53**	**0.15**	**5.93**	**C**	**3.37**	**1.0**	**5.89**	**0.17**
										C	**3.93**	**2.0**	**5.37**	
	2.2	O/N	1.95	2.0	5.46	C	3.38	1.0	5.78	C	3.92	1.0	2.03	0.23
	2.3[h]	*N_{Im}*	*2.01*	*2.0*	*4.88*	*Cu*	*2.52*	*0.2*	*5.97*					*0.45*
3	**3.1**	**O/N**	**1.95**	**2.0**	**5.8**	**Cu**	**2.51**	**0.25**	**5.6**	**C**	**3.94**	**1.5**	**5.0**	**0.14**
	3.2	O/N	1.94	2.0	5.9	C	2.93	1.0	6.8	C	3.95	1.5	4.58	0.20
	3.3[h]	*N_{Im}*	*1.99*	*2.0*	*5.37*	*Cu*	*2.51*	*0.25*	*6.01*					*0.43*
4	**4.1**	**O/N**	**1.96**	**2.0**	**3.94**	**Cu**	**2.52**	**0.2**	**6.01**	**C**	**3.37**	**1.0**	**5.23**	**0.24**
	4.2	O/N	1.96	2.0	3.90	C	2.55	1.0	7.27	C	3.38	1.0	4.77	0.30
	4.3[h]	*N_{Im}*	*2.01*	*2.0*	*3.29*	*Cu*	*2.52*	*0.25*	*5.83*					*0.51*
5	5.1	O/N	1.96	2.0	3.42	Cu	2.53	0.1	5.8	C	3.36	1.0	3.21	0.29
	5.2	**O/N**	**1.96**	**2.0**	**3.37**					**C**	**2.96**	**1.0**	**5.75**	**0.26**
										C	**3.36**	**1.0**	**3.18**	
	5.3[h]	*N_{Im}*	*2.01*	*2.0*	*2.70*									*0.62*

[a] Data were fit over a *k* range of 1 to 12.85 $Å^{-1}$.
[b] Independent metal-ligand scattering environment
[c] Scattering atoms: O (oxygen), N (nitrogen),and C (carbon),
[d] Average metal-ligand bond length from three independent samples
[e] Average metal-ligand coordination number from three independent samples
[f] Average Debye-Waller factor in $Å^2$ x 10^3 from three independent samples
[g] Number of degrees of freedom weighted mean square deviation between data and fit
[h] Fit using both single scattering Feff 7 model with an additional multiple scattering Cu-N(imidazole) model, generated based on crystallographic coordinates, and labeled N_{Im} in table atom designation

Table S3. Size exclusion chromatographic analysis of spmoB and spmoB variants. A peak that elutes at the void volume is not included in the analysis.

Protein	Predicted mass (kDa)	Estimated mass (kDa)
spmoBd1	15.9	26.5 ± 1.8
spmoBd2	16.5	17.3 ± 3.5
spmoB	32.9	38.5 ± 4.1
spmoB_H48N	32.9	35.1 ± 2.8
spmoB_H137,139A	32.7	38.8 ± 1.7
spmoB_H48N_H137,139A	32.7	29.6 ± 1.3

Figure S1. Reversible inhibition of as-isolated pMMO propylene epoxidation activity. **a,** Three equivalents of copper restores 85.4% activity to cyanide-treated pMMO. Retreatment of this sample with cyanide followed by addition of three equivalents of copper again restores 72.6% activity. Although 12 equivalents of copper completely inhibits activity, retreatment of this sample with cyanide followed by addition of three equivalents of copper restores 61.3% activity. **b,** This reversible inhibition is likely the result of hydrogen peroxide formation, the effects of which can be mitigated by addition of catalase (1 mg/ml, data shown in red).

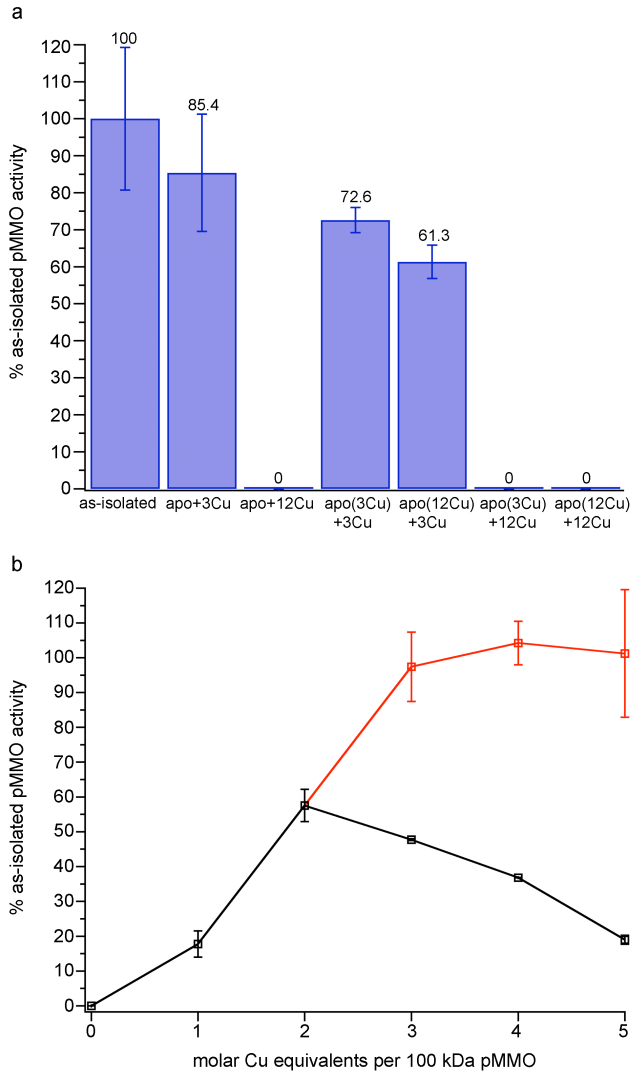

Figure S2. Normalized XANES spectra of sample 1, as-isolated pMMO; sample 2, reconstituted pMMO; sample 3, spmoB; sample 4, spmoB_H48N; sample 5, spmoB_H137,139A. Spectra were offset for clarity. The solid vertical line at ~8984 eV corresponds to the Cu(I) 1s→4p transition.

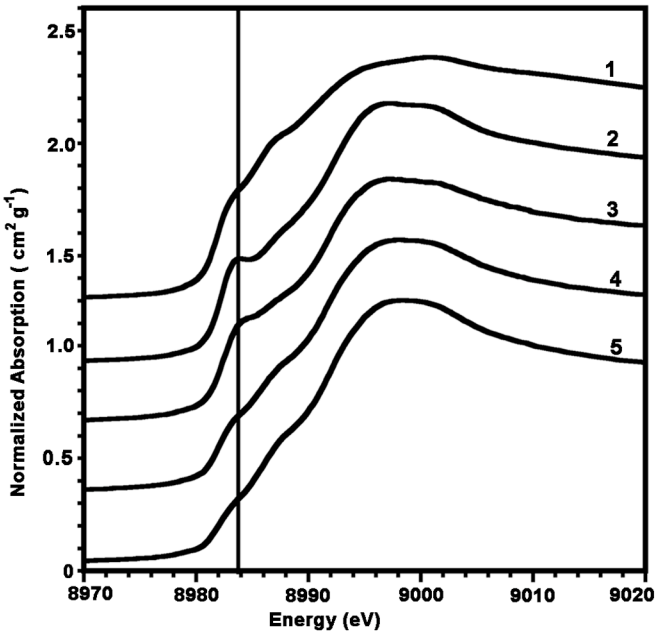

Figure S3. Domain and subunit interfaces in *M. capsulatus* (Bath) pMMO (PDB accession code 1YEW). **a**, Stereoview of selected residues near the domain-domain interface in pmoB. Residues in purple are from the N-terminal cupredoxin domain and are present in the spmoBd1 protein. Residues in green are from the C-terminal cupredoxin domain and are present in the spmoBd2 protein. Residues Phe 41, Arg 43, Arg 45, Trp 49, Asp 51, and Glu 75 from the N-terminal cupredoxin domain are involved in hydrogen bonding interactions with the C-terminal cupredoxin domain. In addition, residues Lys 36, Ala 40, Phe 41, Met 44, Arg 45, His 48, Tyr50, Trp 54, Lys 70, His 72, and Phe 74 make hydrophobic contacts with residues from the C-terminal cupredoxin domain. **b**, Stereoview of selected residues near the dicopper center at the subunit interface between pmoB and pmoC. Residues in purple are from pmoB and residues in light blue are from pmoC. Residues Gly 34, Lys 36, and Ser 37 from pmoB are linked by hydrogen bonds to pmoC residues Asp 166, Asp 79 and Arg 165, respectively. In addition, an interaction surface is formed by His 33, Ser 37, and Trp 136 from pmoB and residues Trp 74, Leu 78, and Phe 81 from pmoC and includes a stacking interaction between the two tryptophan residues.

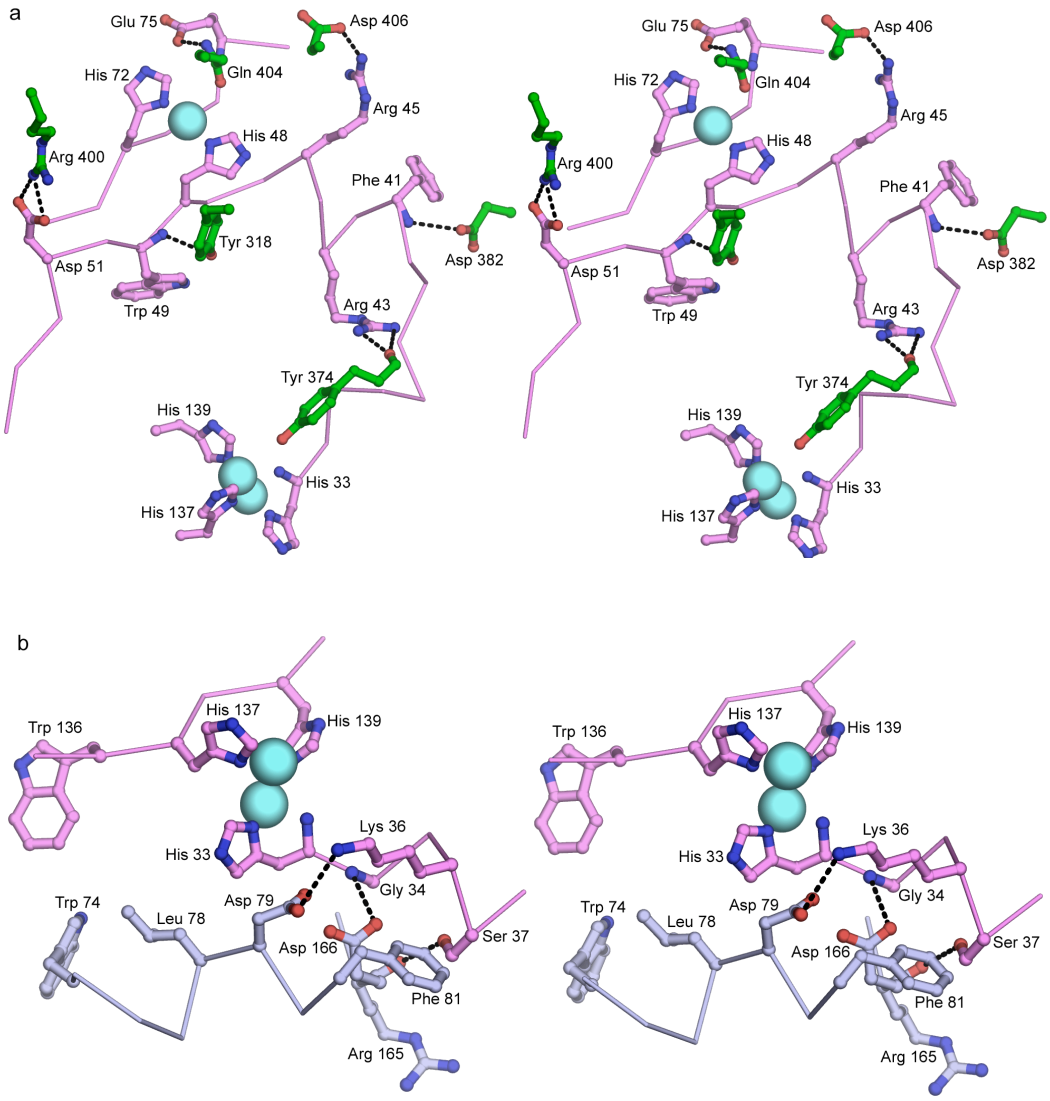

Figure S4. Expression and purification of spmoB. **a**, spmoB and its variants express as inclusion bodies. The proteins were solubilized in a buffer containing 8 M urea and refolded using a dialysis procedure described in the methods section. Molecular mass markers are in lane 7 (kDa). Supernatant-2 and pellet-2 are post detergent washed supernatant and inclusion bodies. **b**, Purified inclusion bodies of spmoB variants. Molecular mass markers in lane 5 are labeled on the right side (kDa).

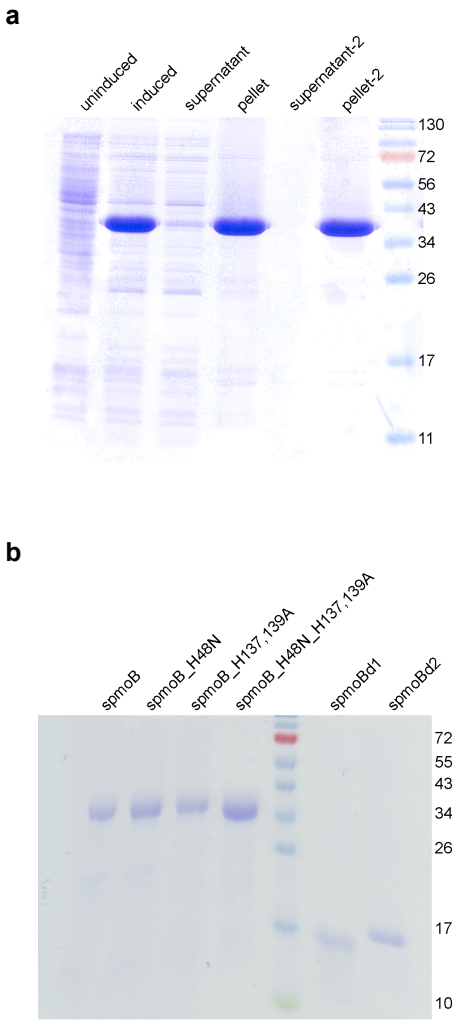

Figure S5. Circular dichroism (CD) spectra of spmoB and its variants. For clarity, CD spectra were scaled to normalize intensities. **a**, Laccase from *Trametes versicolor*. **b**, spmoBd1 (black) and spmoBd2 (red). **c**, spmoB (black), spmoB_H48N (red), spmoB_H137,139A (blue), and spmoB_H48N_H137,139A (green).